NATIONAL ADVISORY COMMITTEE FOR AERONAUTICS

TECHNICAL NOTE 2272

LATERAL ELASTIC INSTABILITY OF HAT-SECTION STRINGERS UNDER COMPRESSIVE LOAD

By Stanley Goodman

National Bureau of Standards

Washington
January 1951

NATIONAL ADVISORY COMMITTEE FOR AERONAUTICS

TECHNICAL NOTE 2272

LATERAL ELASTIC INSTABILITY OF HAT-SECTION STRINGERS UNDER COMPRESSIVE LOAD

By Stanley Goodman

SUMMARY

A strain-energy method is presented for computing the compressive load for lateral elastic instability of hat-section stringers of simple cross section whose side walls and tops are flat and of constant thickness. Buckling stresses for such stringers having five different shapes and a range of lengths were computed by this method. The results confirm an opinion which is already widely held, namely, that lateral instability is an unlikely cause of failure for hat-section stringers.

INTRODUCTION

Hat-section stringers are widely used to reinforce the stressed skin in semimonocoque aircraft structures. They have an advantage over open-section stringers in being much more resistant to lateral instability (instability in which the top of the stringer moves laterally with respect to the base).

Hat-section stringers with thin walls are subject to local instability in which the side walls or tops buckle like plates. Such buckling will usually not prevent the stringer from taking additional load much as a sheet-stringer panel takes additional load after sheet buckles appear.

The failure of the stringer in long panels will be due to Euler column instability. As the length of the stringer is reduced the initial instability may consist of a lateral motion of the top of the stringer. Such instability is likely to be followed immediately by Euler column instability because lateral instability will usually result in a marked decrease in the ability of the top of the stringer to carry additional load and this in turn should markedly lower the effective EI which determines Euler column instability.

Hat-section stringers having the side walls relatively close together tend to approach the cross-sectional shape of open-section stringers. For this reason, it was suspected that in monocoque construction having such hat-section stringers, lateral instability might be the cause of failure. Indications that such was the case for most of the panels of a set tested in compression in a previous investigation were found on inspecting the panels after failure. (See fig. 1.) These panels show evidence of lateral displacement of the tops of the stringers as well as of Euler column instability and local instability of the flanges.

To obtain information regarding the range of dimensions for which lateral instability would be likely for hat-section stringers, it was considered desirable to develop an approximate analysis of this type of buckling for a few stringers with simple cross-sectional shapes. Such an analysis is given in this report for symmetrically shaped hat-section stringers whose tops and side walls are flat. Numerical results are given for five different shapes of stringer cross section.

This investigation was conducted at the National Bureau of Standards under the sponsorship and with the financial assistance of the National Advisory Committee for Aeronautics.

SYMBOLS

$a_1, a_2, \ldots, a_5$ arbitrary constants in stringer deflection equations

D_s flexural rigidity of stringer side walls $\left(\frac{Et_s^3}{12(1 - \mu^2)}\right)$

D_t flexural rigidity of stringer top $\left(\frac{Et_t^3}{12(1 - \mu^2)}\right)$

E Young's modulus

I moment of inertia

G shear modulus $\left(\frac{E}{2(1 + \mu)}\right)$

μ Poisson's ratio; taken as 0.3

h height of stringer side wall (see fig. 2(a))

l length of stringer

M_1	bending moment at root of stringer side wall (see fig. 2(b))
$-M_2$	bending moment at top of stringer side wall (see fig. 2(b))
t_s	thickness of stringer side wall
t_t	thickness of stringer top
w	width of stringer top (see fig. 2(a))
A	cross-sectional area of stringer
x	coordinate along length of stringer (see fig. 2(a))
y	lateral displacement of stringer top (see fig. 2(c))
θ	interior angle between stringer side wall and structure to which stringer is attached (see fig. 2(a))
ξ_s	coordinate along width of stringer side wall (see fig. 2(a))
ξ_t	coordinate along width of stringer top (see fig. 2(a))
σ	axial stress on stringer end
σ_{cr}	critical axial stress
$\sigma_{cr,min}$	critical stress for primary lateral elastic instability of an infinitely long stringer
τ	shear stress

ANALYSIS

A conventional strain-energy method, similar to the method applied to plates on pages 325 to 327 of reference 1 and employing two arbitrary constants in the deflection equations, is used to compute the buckling load for five stringers over a range of lengths. A similar method employing five arbitrary constants in the deflection equations is derived in the appendix, and used to compute buckling loads for various lengths of one of the five stringers. The stringer configuration and displacements (with the corresponding symbols) are shown in figure 2.

Let the lateral displacement of the top y (see fig. 2(c)) be

$$y = a_1 \sin \frac{\pi x}{l} \tag{1}$$

Let the right and left side walls have axial displacements at the top (see fig. 2(d)) U_r and U_l, respectively:

$$U_r = -a_2 \cos \frac{\pi x}{l} \tag{2}$$

$$U_l = a_2 \cos \frac{\pi x}{l} \tag{3}$$

In the top, line 1-1 (fig. 2(c)) rotates clockwise:

$$\frac{dy}{dx} = \frac{a_1 \pi}{l} \cos \frac{\pi x}{l} \tag{4}$$

Line 2-2 rotates clockwise (fig. 2(c)):

$$\frac{U_l - U_r}{w} = \frac{2a_2}{w} \cos \frac{\pi x}{l} \tag{5}$$

The shear strain in the top γ_t is the difference between these two rotations if axial fibers of the top are assumed to remain parallel during the deformation and lines, such as 2-2, to remain straight.

$$\gamma_t = \left(\frac{a_1 \pi}{l} - \frac{2a_2}{w}\right) \cos \frac{\pi x}{l} \tag{6}$$

The shear strains in the right and left side walls γ_r and γ_l, respectively, are similarly

$$\gamma_r = -\frac{U_r}{h} = \frac{a_2}{h} \cos \frac{\pi x}{l} \tag{7}$$

$$\gamma_l = \frac{U_l}{h} = \frac{a_2}{h} \cos \frac{\pi x}{l} \tag{8}$$

The changes in axial stress at the right and left corners $\Delta\sigma_r$ and $\Delta\sigma_l$, respectively, during buckling are:

$$\Delta\sigma_r = E\frac{\partial U_r}{\partial x} = E\frac{a_2\pi}{l}\sin\frac{\pi x}{l} \tag{9}$$

$$\Delta\sigma_l = E\frac{\partial U_l}{\partial x} = -E\frac{a_2\pi}{l}\sin\frac{\pi x}{l} \tag{10}$$

The change in axial stress due to buckling at the clamped edge of the side walls will be taken as zero. Axial stresses will be assumed to vary linearly from edge to edge of the top and each side wall. The change in axial stress $\Delta\sigma_t$ in the top due to buckling is (from equations (9) and (10))

$$\Delta\sigma_t = \frac{2E\xi_t\pi a_2}{wl}\sin\frac{\pi x}{l} \tag{11}$$

The axial strain energy in the top due to buckling V_1 is then

$$V_1 = \frac{t_t}{2E}\int_{-\frac{w}{2}}^{\frac{w}{2}}\int_0^l\left(\frac{2E\xi_t\pi a_2}{wl}\sin\frac{\pi x}{l}\right)^2 dx\, d\xi_t$$

$$= \frac{E\pi^2 a_2{}^2 w t_t}{12l} \tag{12}$$

The change in axial stress $\Delta\sigma_s$ due to buckling for the two side walls is (from equations (9) and (10))

$$\Delta\sigma_s = \frac{E\xi_s\pi a_2}{hl}\sin\frac{\pi x}{l} \tag{13}$$

The strain energy V_2 of the two side walls due to buckling is

$$V_2 = 2 \frac{t_s}{2E} \int_0^h \int_0^l \left(\frac{E\xi_s \pi a_2}{hl} \sin \frac{\pi x}{l}\right)^2 dx\, d\xi_s$$

$$= \frac{E\pi^2 a_2^{\ 2} t_s h}{6l} \tag{14}$$

The strain energy due to buckling stored in shear may be computed as follows: For the top, the shear stress τ_t due to buckling is (from equation (6))

$$\tau_t = G\gamma_t = G\left(\frac{a_1\pi}{l} - \frac{2a_2}{w}\right)\cos \frac{\pi x}{l} \tag{15}$$

The shear strain energy V_3 in the top is then

$$V_3 = \frac{wt_t}{2G} \int_0^l \left[G\left(\frac{a_1\pi}{l} - \frac{2a_2}{w}\right)\cos \frac{\pi x}{l}\right]^2 dx \tag{16}$$

or, taking the shear modulus G as $E/2.6$,

$$V_3 = \frac{Ewlt_t}{10.4}\left(\frac{a_1\pi}{l} - \frac{2a_2}{w}\right)^2 \tag{17}$$

Similarly shear strain energy for the two sides V_4 is (from equations (7) and (8))

$$V_4 = \frac{Et_s l a_2^{\ 2}}{5.2h} \tag{18}$$

For the lateral displacement of the side walls, the following continuity equations must be satisfied: The displacement v at the top of the right side wall (see fig. 2(b)) is, for small displacements,

$$v = \left(a_1 \sin \frac{\pi x}{l}\right)\frac{1}{\sin \theta} \tag{19}$$

The vertical displacement is

$$\left(a_1 \sin \frac{\pi x}{l}\right)\frac{1}{\tan \theta} \tag{20}$$

The change in the angle of the top ψ (fig. 2(b)) is then

$$\psi = \left(a_1 \sin \frac{\pi x}{l}\right)\frac{2}{w \tan \theta} \tag{21}$$

A reasonable approximation to the lateral deflection shape will be obtained by assuming that in the top and side walls the moment varies linearly with ξ_t and ξ_s, respectively, and that the bottom of the side wall has clamped support. This gives

$$D_s \frac{d^2\eta_s}{d\xi_s^{\,2}} = M_1 - \xi_s \frac{M_1 + M_2}{h} \tag{22}$$

Integrating,

$$D_s\eta_s = M_1 \frac{\xi_s^{\,2}}{2} - \frac{\xi_s^{\,3}}{6h}\left(M_1 + M_2\right) \tag{23}$$

where η_s is the lateral deflection of the side due to bending. At the top ξ_s is equal to h, and the lateral deflection of the side η_s is equal to the deflection v of equation (19):

$$\left(a_1 \sin \frac{\pi x}{l}\right)\frac{1}{\sin \theta} = \frac{h^2}{D_s}\left(\frac{M_1}{3} - \frac{M_2}{6}\right) \tag{24}$$

For the top, assuming a linear variation of bending moment and zero moment at the midwidth,

$$D_t \frac{d^2\eta_t}{d\xi_t^{\,2}} = -\frac{2M_2\xi_t}{w} \tag{25}$$

Integrating,

$$D_t\eta_t = -\frac{M_2\xi_t^{\,3}}{3w} + \xi_t(\text{Constant}) \tag{26}$$

where η_t is the deflection of the top due to bending (see fig. 2(b)).

The constant is determined from the condition that the deflection of the top due to bending is equal to zero at the corner. Evaluating the constant and substituting in equation (26) give:

$$D_t\eta_t = -\frac{M_2\xi_t^{\,3}}{3w} + \frac{M_2 w\xi_t}{12} \tag{27}$$

Differentiating,

$$\frac{d\eta_t}{d\xi_t} = -\frac{M_2}{D_t}\left(\frac{\xi_t^{\,2}}{w} - \frac{w}{12}\right) \tag{28}$$

The top at the corner rotates counterclockwise through an angle (from equations (21) and (28)), and

$$\psi + \left(\frac{d\eta_t}{d\xi_t}\right)_{\xi_t=\frac{w}{2}} = \left(a_1 \sin\frac{\pi x}{l}\right)\frac{2}{w\tan\theta} - \frac{M_2 w}{6D_t} \tag{29}$$

where ψ is the change in angle of the top. The side at the corner rotates counterclockwise through an angle $-d\eta_s/d\xi_s$ which may be obtained by differentiating equation (23) and setting ξ_s equal to h. This gives

$$-\left(\frac{d\eta_s}{d\xi_s}\right)_{\xi_s=h} = -\frac{h}{2D_s}\left(M_1 - M_2\right) \tag{30}$$

Equating the rotations of equations (29) and (30),

$$M_1\left(\frac{h}{2D_s}\right) - M_2\left(\frac{w}{6D_t} + \frac{h}{2D_s}\right) = \frac{-2a_1}{w\tan\theta}\sin\frac{\pi x}{l} \tag{31}$$

Solving equations (24) and (31) simultaneously for M_1 and M_2 gives

$$M_1 = \left(\frac{\dfrac{2 \cos \theta}{w} + \dfrac{3}{2h}}{\dfrac{w}{3D_t} + \dfrac{h}{2D_s}} + \frac{3D_s}{h^2}\right)\frac{a_1 \sin \dfrac{\pi x}{l}}{\sin \theta} \tag{32}$$

and

$$M_2 = \left(\frac{\dfrac{2 \cos \theta}{w} + \dfrac{3}{2h}}{\dfrac{w}{3D_t} + \dfrac{h}{2D_s}}\right)\frac{2a_1 \sin \dfrac{\pi x}{l}}{\sin \theta} \tag{33}$$

Expressions may now be obtained for the lateral bending energy and for the energy supplied by the load. From pages 305 to 307 of reference 1 the lateral bending energy V for a plate is

$$V = \frac{D}{2}\iint_R \left(\frac{\partial^2\eta}{\partial\xi^2}\right)^2 + \left(\frac{\partial^2\eta}{\partial x^2}\right)^2 + 2\mu \frac{\partial^2\eta}{\partial\xi^2}\frac{\partial^2\eta}{\partial x^2} + 2(1 - \mu)\left(\frac{\partial^2\eta}{\partial\xi\,\partial x}\right)^2 \tag{34}$$

where D is the flexural rigidity, R is the area of the plate, η is the lateral deflection of the midplane of the plate due to bending, and ξ is the coordinate along the width of the plate. An expression for the lateral bending energy V_5 of the two side walls due to buckling may be obtained by substituting the expressions for M_1 and M_2 (equations (32) and (33)) in equation (23), differentiating η_s with respect to ξ_s and x, substituting the results in equation (34), and integrating. This gives

$$V_5 = a_1^2 D_s\left[\frac{\pi^4}{l^3}\left(0.1K_1^2h^5 - \frac{1}{6}K_1K_2h^6 + \frac{1}{14}K_2^2h^7\right) + l\left(2K_1^2h - 6K_1K_2h^2 + 6K_2^2h^3\right) - \frac{\mu\pi^2}{l}\left(\frac{2}{3}K_1^2h^3 - 2K_1K_2h^4 + 1.2K_2^2h^5\right) + \frac{(1-\mu)\pi^2}{l}\left(\frac{4}{3}K_1^2h^3 - 3K_1K_2h^4 + 1.8K_2^2h^5\right)\right] \tag{35}$$

where

$$K_1 = \frac{1}{2D_s \sin\theta}\left(\frac{\frac{2\cos\theta}{w} + \frac{3}{2h}}{\frac{w}{3D_t} + \frac{h}{2D_s}} + \frac{3D_s}{h^2}\right)$$

$$K_2 = \frac{1}{6hD_s \sin\theta}\left[3\left(\frac{\frac{2\cos\theta}{2} + \frac{3}{2h}}{\frac{w}{3D_t} + \frac{h}{2D_s}}\right) + \frac{3D_s}{h^2}\right]$$

Similarly an expression for the lateral bending energy V_6 of the top due to buckling may be obtained by substituting the expression for M_2 (equation (33)) in equation (27), differentiating η_t with respect to ξ_t and x, substituting the results in equation (34), and integrating. This gives

$$V_6 = a_1^2 D_t\left[\frac{\pi^4}{l^3}\left(\frac{1}{48}K_2^2w^3 - \frac{1}{160}K_3K_4w^5 + \frac{1}{1792}K_4w^7\right) + 0.75lK_4^2w^3 - \frac{\mu\pi^2}{l}\left(-0.25K_3K_4w^3 + \frac{3}{80}K_4^2w^5\right) + \frac{(1-\mu)\pi^2}{l}\left(0.5K_3^2w - 0.25K_3K_4w^3 + \frac{9}{160}K_4^2w^5\right)\right] \tag{36}$$

where

$$K_3 = \frac{w}{6D_t \sin\theta}\left(\frac{\frac{2\cos\theta}{w} + \frac{3}{2h}}{\frac{w}{3D_t} + \frac{h}{2D_s}}\right)$$

$$K_4 = \frac{1}{1.5wD_t \sin\theta}\left(\frac{\frac{2\cos\theta}{w} + \frac{3}{2h}}{\frac{w}{3D_t} + \frac{h}{2D_s}}\right)$$

The strain energy stored during buckling of the stringer will be the sum of the six strain energies derived above.

The energy supplied by the load is the integral over the end cross section of the product of the axial stress and displacement. The part of the axial displacement corresponding to equations (2) and (3) will integrate to zero over the whole cross section. There is an additional axial displacement δ due to lateral sine-wave displacement. From page 28 of reference 1

$$\delta = \frac{\pi^2 d^2}{4l} \tag{37}$$

where d is the lateral displacement at $x = l/2$.

For the side walls, from equations (23), (32), and (33),

$$d = a_1\left(K_1\xi_s^{\,2} - K_2\xi_s^{\,3}\right) \tag{38}$$

where K_1 and K_2 are defined in connection with equation (35).

The energy V_7 expended by the total compressive load on the two side walls is then

$$V_7 = 2\int_0^h \sigma t_s \frac{a_1^{\,2}\pi^2}{4l}\left(K_1\xi_s^{\,2} - K_2\xi_s^{\,3}\right)^2 d\xi_s$$

$$= \frac{\sigma a_1^{\,2}\pi^2 t_s}{l}\left(0.1K_1^{\,2}h^5 - \frac{1}{6}K_1K_2h^6 + \frac{1}{14}K_2^{\,2}h^7\right) \tag{39}$$

For the top, the maximum horizontal displacement is a_1 (equation 1) and the maximum vertical displacement for small displacements is given by equations (21), (27), and (33). From these d^2 may be obtained as:

$$d^2 = a_1^2\left[1 + \left(K_3\xi_t - K_4\xi_t^3 + \frac{2\xi_t}{w \tan\theta}\right)^2\right] \tag{40}$$

where

$$K_3 = \frac{w}{6D_t \sin\theta}\left(\frac{\frac{2\cos\theta}{w} + \frac{3}{2h}}{\frac{w}{3D_t} + \frac{h}{2D_s}}\right)$$

$$K_4 = \frac{1}{1.5wD_t \sin\theta}\left(\frac{\frac{2\cos\theta}{w} + \frac{3}{2h}}{\frac{w}{3D_t} + \frac{h}{2D_s}}\right)$$

and the energy V_8 expended by the external compressive load on the top is then

$$V_8 = \int_{-\frac{w}{2}}^{\frac{w}{2}} \frac{\sigma t_t \pi^2}{4l} d^2 \, d\xi_t$$

$$= \sigma \frac{a_1^2\pi^2 t_t}{4l}\left[w + \frac{1}{12} K_3^2 w^3 - \frac{1}{40} K_3K_4w^5 + \frac{1}{448} K_4^2 w^7 + \right.$$

$$\left. \frac{1}{\tan\theta}\left(\frac{1}{3} K_3w^2 - \frac{1}{20} K_4w^4 + \frac{w}{3\tan\theta}\right)\right] \tag{41}$$

At the buckling load, the energy put in equals the strain energy stored. Equating the strain energy stored (equations (12), (14), (17), (18), (35), and (36)) to the energy put in (equations (39) and (41)) and solving for the critical axial stress σ_{cr} as a function of a_2/a_1 give

$$\sigma_{cr} = \frac{\dfrac{t_t E\pi^2 w}{10.4l} + \dfrac{1}{a_1{}^2} V_5 + \dfrac{1}{a^2} V_6}{\dfrac{1}{a_1{}^2\sigma_{cr}}\left(V_7 + V_8\right)} - \frac{\left(\dfrac{\pi t_t E}{2.6}\right)\left(\dfrac{a_2}{a_1}\right) + \left(\dfrac{1}{a_2{}^2} V_1 + \dfrac{1}{a_2{}^2} V_2 + \dfrac{1}{a_2{}^2} V_4 + \dfrac{t_t E}{2.6w}\right)\left(\dfrac{a_2}{a_1}\right)^2}{\dfrac{1}{a_1{}^2\sigma_{cr}}\left(V_7 + V_8\right)} \tag{42}$$

The value of a_2/a_1 for which σ_{cr} is a minimum is

$$\frac{a_2}{a_1} = \frac{1}{2}\,\frac{\dfrac{\pi t_t E}{2.6}}{\dfrac{1}{a_2{}^2} V_1 + \dfrac{1}{a_2{}^2} V_2 + \dfrac{1}{a_2{}^2} V_4 + \dfrac{t_t E l w}{2.6}} \tag{43}$$

Substituting the expression for a_2/a_1 of equation (43) in equation (42) gives

$$\sigma_{cr} = \frac{1}{\dfrac{1}{a_1{}^2\sigma_{cr}}\left(V_7 + V_8\right)}\left[\frac{t_t E\pi^2 w}{10.4l} + \frac{1}{a_1{}^2} V_5 + \frac{1}{a_1{}^2} V_6 - \frac{\pi^2 t_t{}^2 E^2}{27.04\left(\dfrac{1}{a_2{}^2} V_1 + \dfrac{1}{a_2{}^2} V_2 + \dfrac{1}{a_2{}^2} V_4 + \dfrac{t_t E l}{2.6w}\right)}\right] \tag{44}$$

where

V_1 axial strain energy due to buckling in the top (equation (12))

V_2 axial strain energy due to buckling in the two side walls (equation (14))

V_3 shear strain energy due to buckling in the top (equation (17))

V_4 shear strain energy due to buckling in the two side walls (equation (18))

V_5 bending strain energy due to buckling in the two side walls (equation (35))

V_6 bending strain energy due to buckling in the top (equation (36))

V_7 energy expended by external compressive load on the two side walls (equation (39))

V_8 energy expended by external compressive load on the top (equation (41))

The quantities a_1, a_2, and σ_{cr} on the right-hand side of equation (44) will cancel out of the equation when the expressions for the strain energy are substituted, leaving an expression for σ_{cr} in terms of E, μ, and the stringer dimensions. A critical-strain ratio σ_{cr}/E may be obtained by dividing through equation (44) by E.

SHAPE OF STRINGERS ANALYZED

Stringers of five cross-sectional shapes were analyzed. They include three with side walls and tops of equal thickness and two with the top thickness 2.24 times the side wall thickness. Four had side walls perpendicular to the structure to which they were attached, and one had an interior angle of 64.2° between the side wall and structure. Shapes of the stringers drawn to scale of equal area are presented in figure 3, and the dimensions of the stringers are given in columns (2) to (5) of table 1. Sections 1 and 2 approximate stringers currently used, while sections 3, 4, and 5 are variations of section 1 chosen to show the effect of changes in height and wall thickness.

PRIMARY BUCKLING STRENGTH OF STRINGERS

The critical-strain ratio σ_{cr}/E plotted against the length ratio $l/\sqrt{A}$ for the five stringer shapes analyzed is presented in figure 4. The ratio $l/\sqrt{A}$ was chosen as abscissa since it has a fixed value for all geometrically similar specimens and also a fixed value for all geometrically different specimens of a given length having the same cross-sectional area. Comparison of ordinates for a given abscissa will therefore show the effect of changing the distribution of material in the flange. The buckling-stress ratios in figure 4 decrease with increasing stringer length, go through a minimum $\sigma_{cr,min}/E$ at a flange length less than that usually encountered in aircraft structures, and then increase for greater stringer lengths. A relatively long stringer with simply supported loaded ends will buckle into half sine waves, the number of which may be determined by following the procedure for plates described on page 330 of reference 1. It is apparent from the curves in figure 4 that, using this procedure, the buckling-stress ratio for a long stringer $\left(l > 25\sqrt{A}\right)$ will be close to $\sigma_{cr,min}/E$. Values of $\sigma_{cr,min}/E$ are listed in column (6) of table 1. They range from 0.0141 to 0.0444, indicating that, for aircraft materials, buckling would occur in the plastic range. Since the buckling-strain ratios obtained appeared to be high, a similar method of analysis using five arbitrary constants in the deflection equations and assuming hinged support for the side walls at the root was derived. This method is presented in the appendix. Buckling-strain ratios were computed for section 1 by this method, and are plotted against the length ratio in figure 4. The value of $\sigma_{cr,min}/E$ (column (7), table 1) obtained by the second method was 34 percent lower than that obtained by the first method. This indicates the need for using the solution involving five arbitrary constants where greater accuracy is desired.

STRINGER DEFLECTION SHAPES

Expressions for the relative transverse deflection shape of the stringers may be obtained from the method of analysis using two arbitrary constants by assuming a value of unity for a_1 and substituting values of the bending moments from equations (32) and (33) in the deflection equations (23) and (27). The lateral deflection shapes of the right sides of stringer sections 1 and 2 so obtained are presented in figure 5. Relative displacements of the stringer elements corresponding to equation (19) and equations (A2) and (A3) in the appendix may be obtained from the method of analysis using five arbitrary constants (presented in the appendix) by assuming a value of unity for a_1, arbitrarily selecting four of equations (A35), substituting the buckling-strain ratio for σ_{cr}/E, and solving the resulting equations simultaneously for a_2, a_3, a_4, and a_5. The relative deflections may then be obtained by substituting the values of the constants in equations (A1), (A2), and (A3). The relative lateral transverse deflections of the stringer side wall and top, assuming hinged support at the stringer root, may be obtained by assuming a value for a_1, obtaining the values of M_1

by substituting the value of a_1 in equation (A25), substituting these values in equations (A21) and (A23), and solving these equations for η_s and η_t. The lateral deflection shape of the right side of stringer section 1 is presented in figure 6.

CONCLUDING REMARKS

The high values of computed elastic strain for lateral instability for the five stringer sections investigated substantiate the widely held opinion that closed-section stringers of reasonable proportions fail in ways other than lateral instability of the top. Even in the case of the narrowest section, $\sigma_{cr,min}/E$ is 0.0141, a value well into the plastic range for aluminum alloys.

National Bureau of Standards
Washington, D. C., August 11, 1949

APPENDIX

STRAIN-ENERGY METHOD FOR COMPUTING BUCKLING-STRAIN RATIO USING FIVE ARBITRARY CONSTANTS IN DEFLECTION EQUATIONS

Let the lateral deflection of the top be

$$y = a_1 \sin \frac{\pi x}{l} \tag{A1}$$

Let the axial deflection of the top be

$$u_t = -\left[a_2 \frac{2h}{w} \xi_t - a_3 \xi_t \left(\frac{w^2}{4} - \xi_t{}^2\right)\right] \cos \frac{\pi x}{l} \tag{A2}$$

An expression for the axial deflection of the right side wall which coincides at the corner with the axial deflections given by equation (A2) is

$$u_r = -\left[a_2 \xi_s + a_4 \xi_s \left(\frac{\xi_s}{h} - 1\right) + a_5 \xi_s{}^2 \left(\frac{\xi_s}{h} - 1\right)\right] \cos \frac{\pi x}{l} \tag{A3}$$

Let the axial deflection of the left side wall be

$$u_l = -u_r \tag{A4}$$

It is further assumed that axial fibers in the top remain parallel to each other. A similar assumption applies to the side walls.

The shear strain in the top γ_t is then

$$\gamma_t = \frac{\partial y}{\partial x} + \frac{\partial u_t}{\partial \xi_t} = \left(a_1 \frac{\pi}{l} - a_2 \frac{2h}{w} + a_3 \frac{w^2}{4} - 3a_3 \xi_t{}^2\right) \cos \frac{\pi x}{l} \tag{A5}$$

Shear strain in the right side wall γ_r is

$$\gamma_r = \frac{\partial u_r}{\partial \xi_s} + \frac{\partial v_r}{\partial x} = -\left[a_2 + a_4\left(\frac{2\xi_s}{h} - 1\right) + a_5\left(\frac{3\xi_s^{\,2}}{h} - 2\xi_s\right)\right]\cos\frac{\pi x}{l} \tag{A6}$$

where v_r is the deflection of the right side wall in the ξ_s-direction and equals zero.

Shear strain in the left side wall γ_l is

$$\gamma_l = -\gamma_r \tag{A7}$$

The change in axial stress $\Delta\sigma_t$ in the top due to buckling is

$$\begin{aligned}\Delta\sigma_t &= \frac{E}{1 - \mu^2}\,\epsilon_t \\ &= \frac{E}{1 - \mu^2}\,\frac{\partial u_t}{\partial x} \\ &= \left[a_2\,\frac{2h}{w}\,\xi_t - a_3\left(\frac{w^2}{4} - \xi_t^{\,2}\right)\xi_t\right]\left[\frac{\pi E}{l\left(1 - \mu^2\right)}\sin\frac{\pi x}{l}\right]\end{aligned} \tag{A8}$$

where ϵ_t is the axial strain.

The change in axial stress $\Delta\sigma_r$ in the right side wall due to buckling is

$$\begin{aligned}\Delta\sigma_r &= \frac{E}{1 - \mu^2}\,\frac{\partial u_r}{\partial x} \\ &= \left[a_2\xi_s + a_4\xi_s\left(\frac{\xi_s}{h} - 1\right) + a_5\xi_s^{\,2}\left(\frac{\xi_s}{h} - 1\right)\right]\left[\frac{\pi E}{l\left(1 - \mu^2\right)}\sin\frac{\pi x}{l}\right]\end{aligned} \tag{A9}$$

The axial strain energy V_1 in the top due to buckling is (from equation (A8))

$$V_1 = \frac{t_t \pi^2 E}{4l\left(1 - \mu^2\right)^2}\left(\frac{1}{3} h^2 w a_2{}^2 - \frac{1}{30} h w^4 a_2 a_3 + 0.0011905 w^7 a_3{}^2\right) \tag{A10}$$

The axial strain energy V_2 in the two sides due to buckling is (from equation (A9))

$$V_2 = \frac{t_s \pi^2 E}{2\left(1 - \mu^2\right)^2}\left(\frac{1}{3} h^3 a_2{}^2 - \frac{1}{6} h^3 a_2 a_4 - \frac{1}{10} h^4 a_2 a_5 + \frac{1}{30} h^3 a_4{}^2 + \frac{1}{30} h^4 a_4 a_5 + \frac{1}{105} h^5 a_5{}^2\right) \tag{A11}$$

The change in transverse stress $\Delta\sigma_{\xi_t}$ in the top is

$$\Delta\sigma_{\xi_t} = \frac{\mu E}{1 - \mu^2} \varepsilon_t = \mu \Delta\sigma_t \tag{A12}$$

The strain energy V_{1a} in the top due to transverse compressive stress is (from equation (A12))

$$V_{1a} = \int_{\text{volume}} \frac{\left(\mu \Delta\sigma_t\right)^2}{2E} = \mu^2 V_1 \tag{A13}$$

Similarly the strain energy V_{2a} in the two side walls due to transverse compressive stress is

$$V_{2a} = \mu^2 V_2 \tag{A14}$$

Shear strain energy due to buckling is given by

$$\int_{\text{volume}} \frac{\tau^2}{2G} \tag{A15}$$

Shear strain energy V_3 in the top due to buckling is (from equations (A5) and (A15))

$$V_3 = \frac{t_t E}{8(1 + \mu)}\left(\frac{\pi^2 w}{l} a_1^2 - 4\pi h a_1 a_2 + \frac{4h^2 l}{w} a_2^2 + \frac{l w^5}{20} a_3^2\right) \tag{A16}$$

The shear strain energy V_4 in the two side walls due to buckling is (from equations (A6) and (A15))

$$V_4 = \frac{t_s E l}{4(1 + \mu)}\left(h a_2^2 + \frac{1}{3} h a_4^2 + \frac{1}{3} h^2 a_4 a_5 + \frac{2}{15} h^3 a_5^2\right) \tag{A17}$$

The displacement v (fig. 2(b)) at the top of the right side wall is

$$v = \left(a_1 \sin \frac{\pi x}{l}\right)\frac{1}{\sin \theta} \tag{A18}$$

The change in the angle of the top ψ is

$$\psi = \left(a_1 \sin \frac{\pi x}{l}\right)\frac{2}{w \tan \theta} \tag{A19}$$

A reasonable approximation of the lateral deflection shape may be obtained by assuming that the moment varies linearly with ξ_t and ξ_s in the top and side walls, respectively. Assuming hinged support at the root of the side wall, $M_1 = 0$. Then, for the side wall

$$D_s \frac{d^2\eta_s}{d{\xi_s}^2} = -M_2 \frac{\xi_s}{h} \tag{A20}$$

where η_s is the lateral deflection of the side wall due to bending.

Integrating equation (A20) and obtaining the values of the constants of integration from the conditions that $\eta_s = 0$ at $\xi_s = 0$, and $\eta_s = v$ (displacement at the top of the side wall; see equation (A18)) at $\xi_s = h$ give

$$D_s\eta_s = -M_2\left(\frac{\xi_s{}^3}{6h} - \frac{h\xi_s}{6}\right) + a_1\left(\sin\frac{\pi x}{l}\right)\frac{D_s\xi_s}{h \sin\theta} \tag{A21}$$

For the top

$$D_t\frac{d^2\eta_t}{d\xi_t{}^2} = -M_2\frac{2\xi_t}{w} \tag{A22}$$

where η_t is the lateral deflection of the top due to bending.

Integrating equation (A22) and evaluating the constants of integration from the condition that the deflection of the top due to bending is zero at $\xi_t = 0$ and $\xi_t = w/2$ give

$$D_t\eta_t = -\frac{M_2\xi_t{}^3}{3w} + \frac{M_2 w\xi_t}{12} \tag{A23}$$

The moment M_2 may be obtained by equating the counterclockwise rotations of the top and side wall at the corner

$$\psi + \left(\frac{d\eta_t}{d\xi_t}\right)_{\xi_t=\frac{w}{2}} = -\left(\frac{d\eta_s}{d\xi_s}\right)_{\xi_s=h} \tag{A24}$$

Substituting the expressions for ψ, $\left(d\eta_t/d\xi_t\right)_{\xi_t=\frac{w}{2}}$, and $\left(d\eta_s/d\xi_s\right)_{\xi_s=h}$ obtained from equations (A19), (A23), and (A21) in equation (A24) and solving for M_2 give

$$M_2 = \frac{\left(a_1 \sin\frac{\pi x}{l}\right)\left(\frac{2}{w \tan\theta} + \frac{1}{h \sin\theta}\right)}{\frac{w}{6D_t} + \frac{h}{3D_s}} \tag{A25}$$

The energy V of a plate due to lateral bending is (from reference 1, pp. 305-307)

$$V = \frac{D}{2}\iint_R \left(\frac{\partial^2\eta}{\partial\xi^2}\right)^2 + \left(\frac{\partial^2\eta}{\partial x^2}\right)^2 + 2\mu \frac{\partial^2\eta}{\partial x^2}\frac{\partial^2\eta}{\partial\xi^2} + 2(1 - \mu)\left(\frac{\partial^2\eta}{\partial\xi\partial x}\right)^2 \tag{A26}$$

where R is the area of the plate and η is the deflection of the midplane of the plate due to bending.

Substituting the values of the derivatives of η_s with respect to ξ_s and x obtained from equation (A21) in equation (A26) and integrating give for the lateral bending strain energy V_5 of the side walls due to buckling

$$V_5 = a_1{}^2D_s\left[\frac{\pi^4}{2l^3}\left(\frac{1}{3}K_1{}^2h^3 - 0.4K_1K_2h^5 + \frac{1}{7}K_2{}^2h^7\right) + 6lK_2{}^2h^3 + \right.$$
$$\left.\frac{2\mu\pi^2}{l}\left(K_1K_2h^3 - 0.6K_2{}^2h^5\right) + \frac{(1 - \mu)\pi^2}{l}\left(K_1{}^2h - 2K_1K_2h^3 + 1.8K_2{}^2h^5\right)\right] \tag{A27}$$

where

$$K_1 = \frac{1}{h \sin\theta} + \frac{h}{6D_s}\,\frac{\dfrac{2}{w\tan\theta} + \dfrac{1}{h\sin\theta}}{\dfrac{w}{6D_t} + \dfrac{h}{3D_s}}$$

$$K_2 = \frac{1}{6hD_s}\,\frac{\dfrac{2}{w\tan\theta} + \dfrac{1}{h\sin\theta}}{\dfrac{w}{6D_t} + \dfrac{h}{3D_s}}$$

Similarly an expression for the lateral bending strain energy V_6 in the top due to buckling may be obtained from equations (A23), (A25), and (A26):

$$V_6 = a_1^2 \frac{D_t}{2}\left[\frac{\pi^4}{l^3}\left(\frac{1}{24} K_3^2w^3 - \frac{1}{80} K_3K_4w^5 + \frac{1}{896} K_4^2w^7\right) + 1.5K_4^2w^3l - \right.$$

$$\frac{2\mu\pi^2}{l}\left(-0.25K_3K_4w^3 + \frac{3}{80} K_4^2w^5\right) +$$

$$\left.\frac{(1 - \mu)\pi^2}{l}\left(K_3^2w - 0.5K_3K_4w^3 + \frac{9}{80} K_4^2w^5\right)\right] \tag{A28}$$

where

$$\left.\begin{aligned} K_3 &= \frac{w}{12D_t}\left(\frac{\frac{2}{w \tan \theta} + \frac{1}{h \sin \theta}}{\frac{w}{6D_t} + \frac{h}{3D_s}}\right) \\ K_4 &= \frac{1}{3wD_t}\left(\frac{\frac{2}{w \tan \theta} + \frac{1}{h \sin \theta}}{\frac{w}{6D_t} + \frac{h}{3D_s}}\right) \end{aligned}\right\} \tag{A29}$$

The strain energy of the stringer due to buckling is the sum of the strain energies V_1 to V_6 derived above.

The energy supplied by the load is the integral over the end cross section of the product of the axial stress and axial displacement. The part of the axial displacements corresponding to equations (A2), (A3), and (A4) will integrate to zero over the ends, since the displacement of the top is antisymmetric about the center line, and displacements of the right and left side walls are equal and opposite. The end displacement due to lateral sine-wave displacement δ is (reference 1, p. 28)

$$\delta = \frac{\pi^2 d^2}{4l} \tag{A30}$$

where d is the lateral displacement at $x = l/2$.

The energy V_7 for the two side walls may be obtained by substituting an expression for d of the side walls (obtainable from equations (A21) and (A25)) in equation (A30), and integrating the product of the axial stress and end displacement over the side-wall ends. This gives

$$V_7 = 2\int_0^h \frac{\sigma\pi^2}{4l} d^2 t_s \, d\xi_s = a_1^2 \frac{\sigma\pi^2 t_s}{2l}\left(\frac{1}{3} K_1^2 h^3 - 0.4K_1K_2h^5 + \frac{1}{7} K_2^2 h^7\right) \tag{A31}$$

where K_1 and K_2 are defined in connection with equation (A27).

Values of d^2 for the stringer top may be obtained from equations (A1) (horizontal component) and (A23), (A25), and (A18) (vertical component)

$$d^2 = a_1^2 + \left[a_1\left(K_3\xi_t - K_4\xi_t^3 + \frac{2\xi_t}{w \tan \theta}\right)\right]^2 \tag{A32}$$

where K_3 and K_4 are defined by equations (A29).

The energy V_8 for the top may be obtained from equations (A30) and (A32) by integrating the product of the axial stress and the displacement over the end cross section of the top. This gives

$$V_8 = \int_{-\frac{w}{2}}^{\frac{w}{2}} \frac{\pi^2\sigma_x t_t}{4l} d_t^2 \, d\xi_t$$

$$= \left[w + \frac{1}{12} K_3^2 w^3 - 0.025K_3K_4w^5 + \frac{1}{448} K_4^2 w^7 + \frac{1}{\tan \theta}\left(\frac{1}{3} K_3 w^2 - 0.025K_4 w^4 + \frac{w}{3 \tan \theta}\right)\right]\frac{a_1^2\pi^2 t_t \sigma_x}{4l} \tag{A33}$$

where σ_x is the stress in the x-direction.

The work of the external forces in producing buckling is the sum of the energy for the side walls V_7 and for the top V_8.

The critical buckling load may be obtained by the method outlined on pages 325 to 327 of reference 1 as follows:

The work of the external forces is $I_2\sigma$ or

$$I_2 = \text{Work of external forces}/\sigma$$

The strain energy of the stringer I_1 is the sum of the previously derived strain energies V_1 to V_6. The critical stress is given by

$$I_2\sigma_{cr} = I_1$$

or

$$\frac{\sigma_{cr}}{E} = \frac{I_1/E}{I_2} \tag{A34}$$

Values of the constants must be such as to give the lowest possible value of buckling stress. This condition will be satisfied if the constants satisfy the set of simultaneous equations

$$\left.\begin{aligned} \frac{\partial I_1/E}{\partial a_1} + \frac{\sigma_{cr}}{E}\frac{\partial I_2}{\partial a_1} &= 0 \\ \frac{\partial I_1/E}{\partial a_2} + \frac{\sigma_{cr}}{E}\frac{\partial I_2}{\partial a_2} &= 0 \\ \cdot\ \cdot\ \cdot\ \cdot\ \cdot\ \cdot\ \cdot& \end{aligned}\right\} \tag{A35}$$

Solutions of equations (A35) may be obtained only if the determinant of the equations is equal to zero. The critical-strain ratio σ_{cr}/E may be obtained by substituting the expressions obtained for I_1/E and I_2 in equation (A35), setting the determinant of the resulting equations equal to zero, and solving for the lowest value of σ_{cr}/E. The critical-strain ratio appears in only one term of the determinant. This term may be relegated to the last row, last column of the determinant. The determinant may be solved with a minimum of effort by the Crout method (reference 2). The solution, which contains the critical buckling-strain ratio, may then be set equal to zero and solved for the value of the critical-strain ratio.

REFERENCES

1. Timoshenko, S.: Theory of Elastic Stability. First ed., McGraw-Hill Book Co., Inc. 1936.

2. Crout, Prescott D.: A Short Method for Evaluating Determinants and Solving Systems of Linear Equations with Real or Complex Coefficients. Trans. AIEE, vol. 60, June 1941, pp. 1235-1240.

TABLE I

DIMENSIONS AND CRITICAL-STRAIN RATIOS OF

STRINGERS ANALYZED

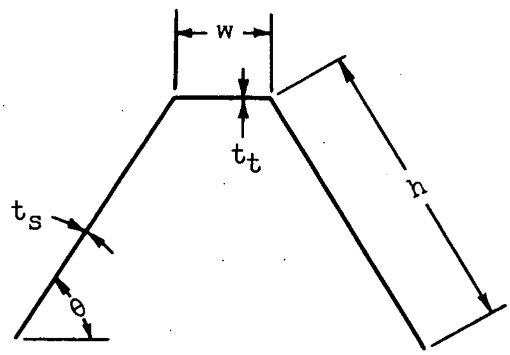

(1)	(2)	(3)	(4)	(5)	(6)	(7)
Stringer	$\frac{h}{t_s}$	$\frac{w}{t_s}$	$\frac{t_t}{t_s}$	θ (deg)	$\frac{\sigma_{cr,min}}{E}$ (1)	$\frac{\sigma_{cr,min}}{E}$ (2)
1	18.25	7.250	1	90	0.0444	0.0294
2	21.26	7.276	2.244	64.2	.0307	------
3	37.00	7.250	1	90	.0141	------
4	21.26	7.276	2.244	90	.0284	------
5	14.80	2.900	1	90	.0252	------

[1]Method employing two arbitrary constants in deflection equations; side walls assumed clamped at root.

[2]Method employing five arbitrary constants in deflection equations; side walls assumed hinged at root.

Page intentionally left blank

Page intentionally left blank

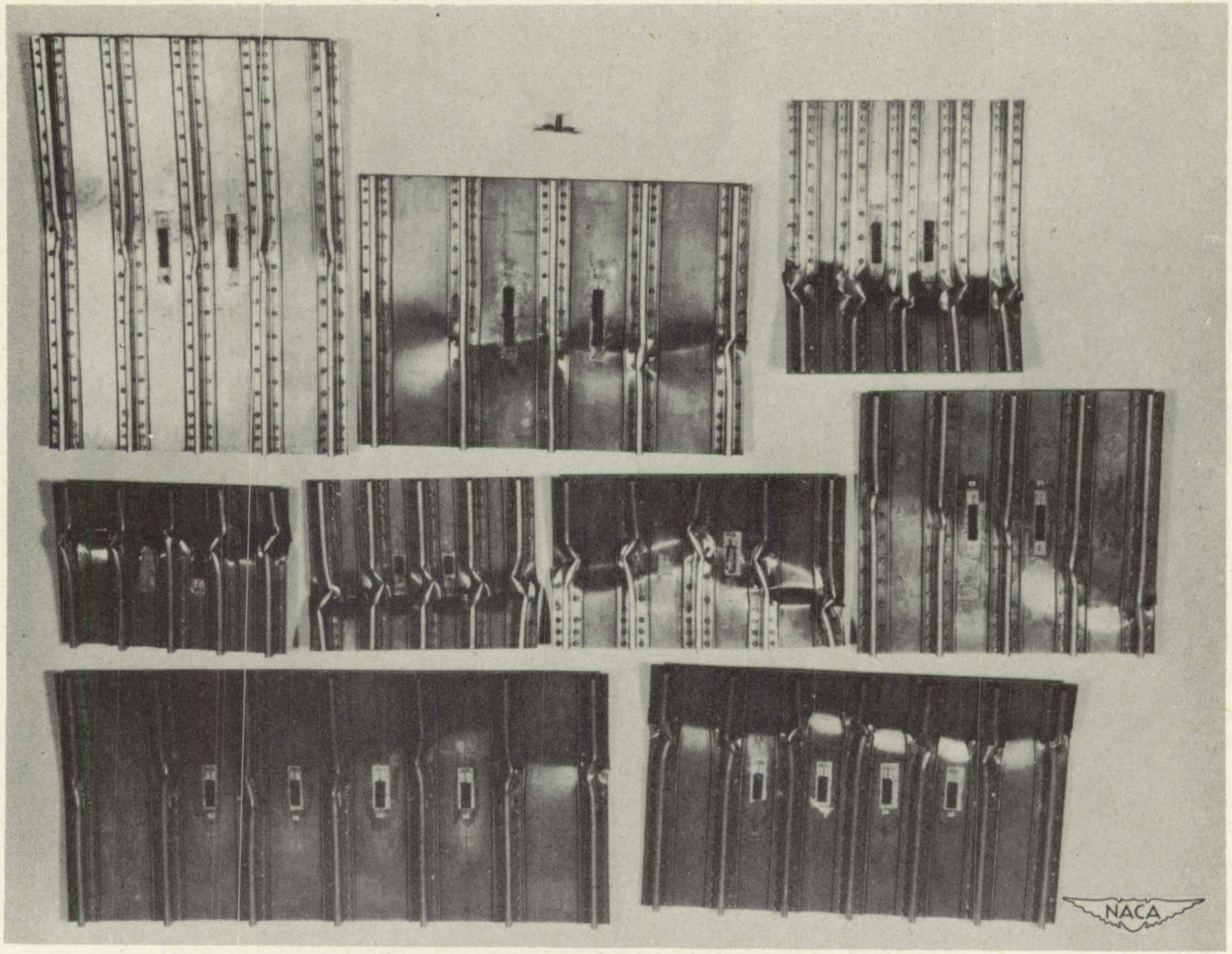

Figure 1.- Sheet-stringer panels from a previous investigation showing lateral displacement of stringer tops. Stringers had closely spaced side walls as can be seen from stringer cross section in center top of figure.

Page intentionally left blank

Page intentionally left blank

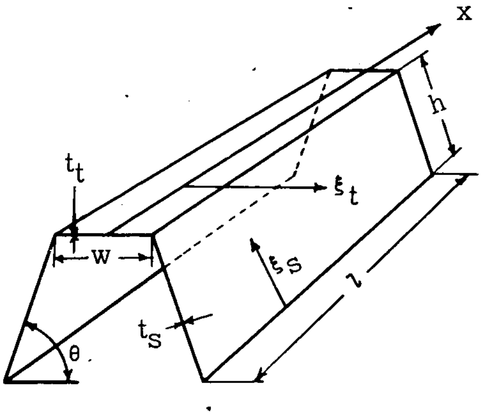

(a) Stringer.

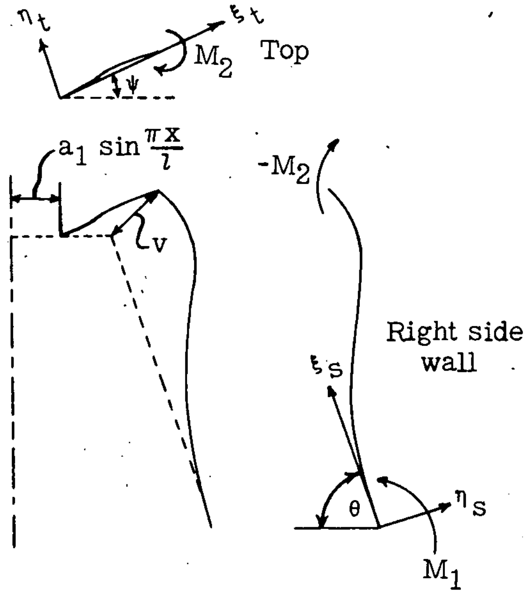

(b) Lateral displacements of top and right side wall during buckling.

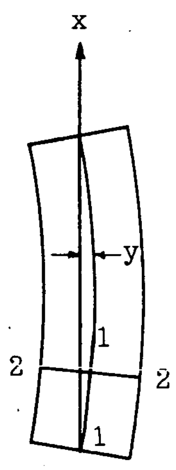

(c) Stringer top during buckling.

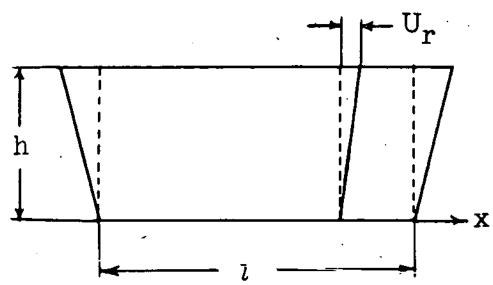

(d) Axial displacements of right side wall during buckling.

Figure 2.- Stringer configuration and displacements.

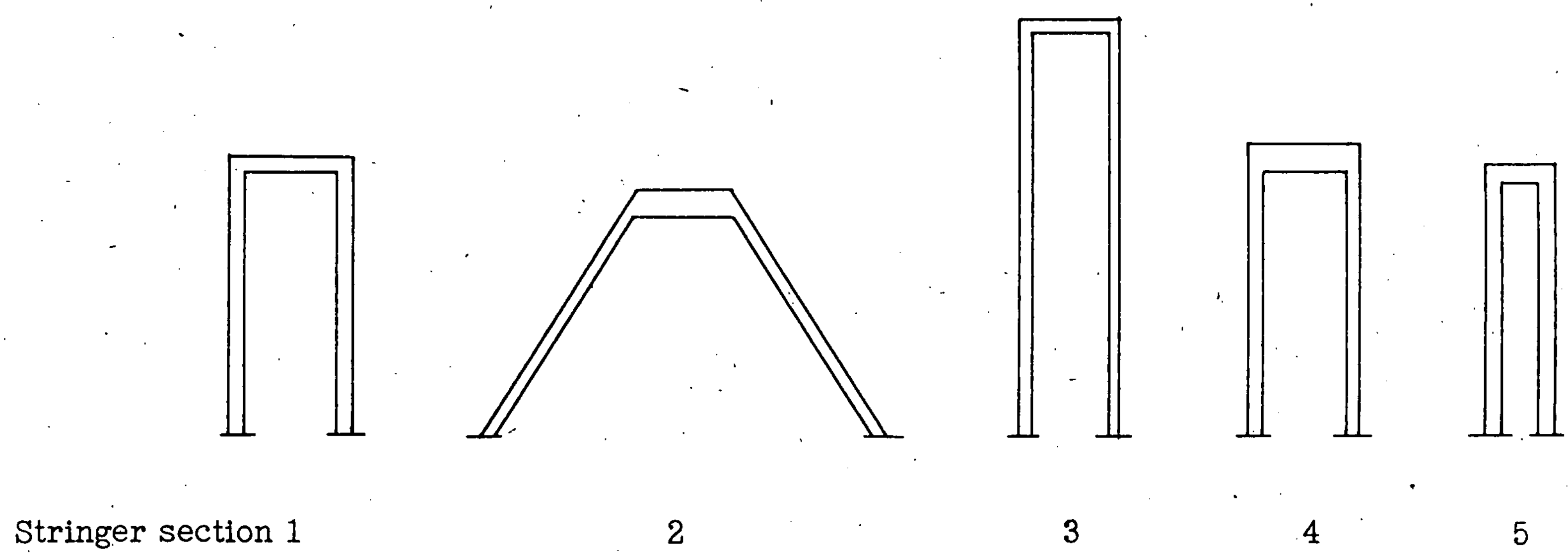

Figure 3.- Shape of stringers analyzed drawn to scale of equal area. (See table 1 for dimensions.)

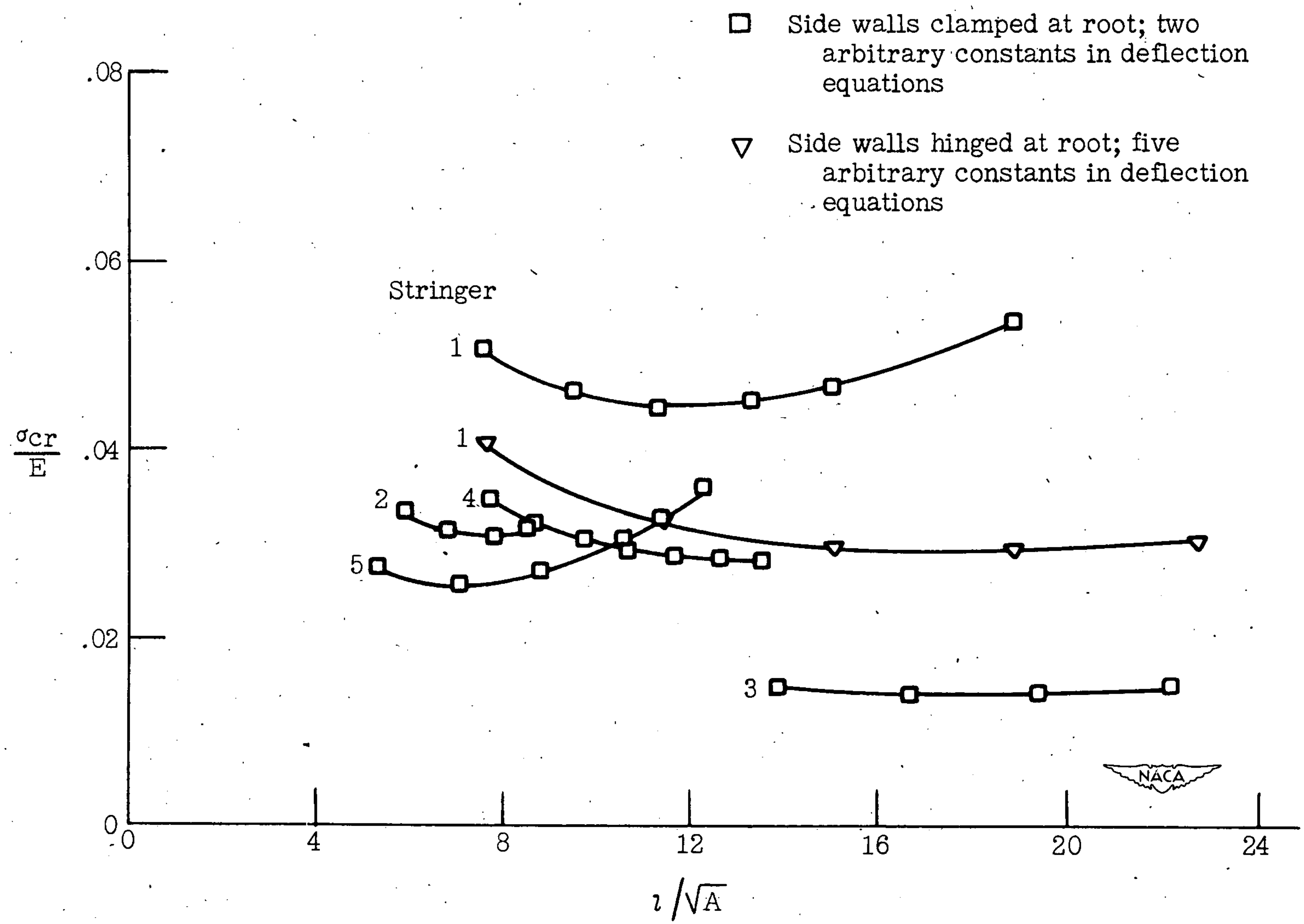

Figure 4.- Primary lateral elastic buckling strength of stringers.

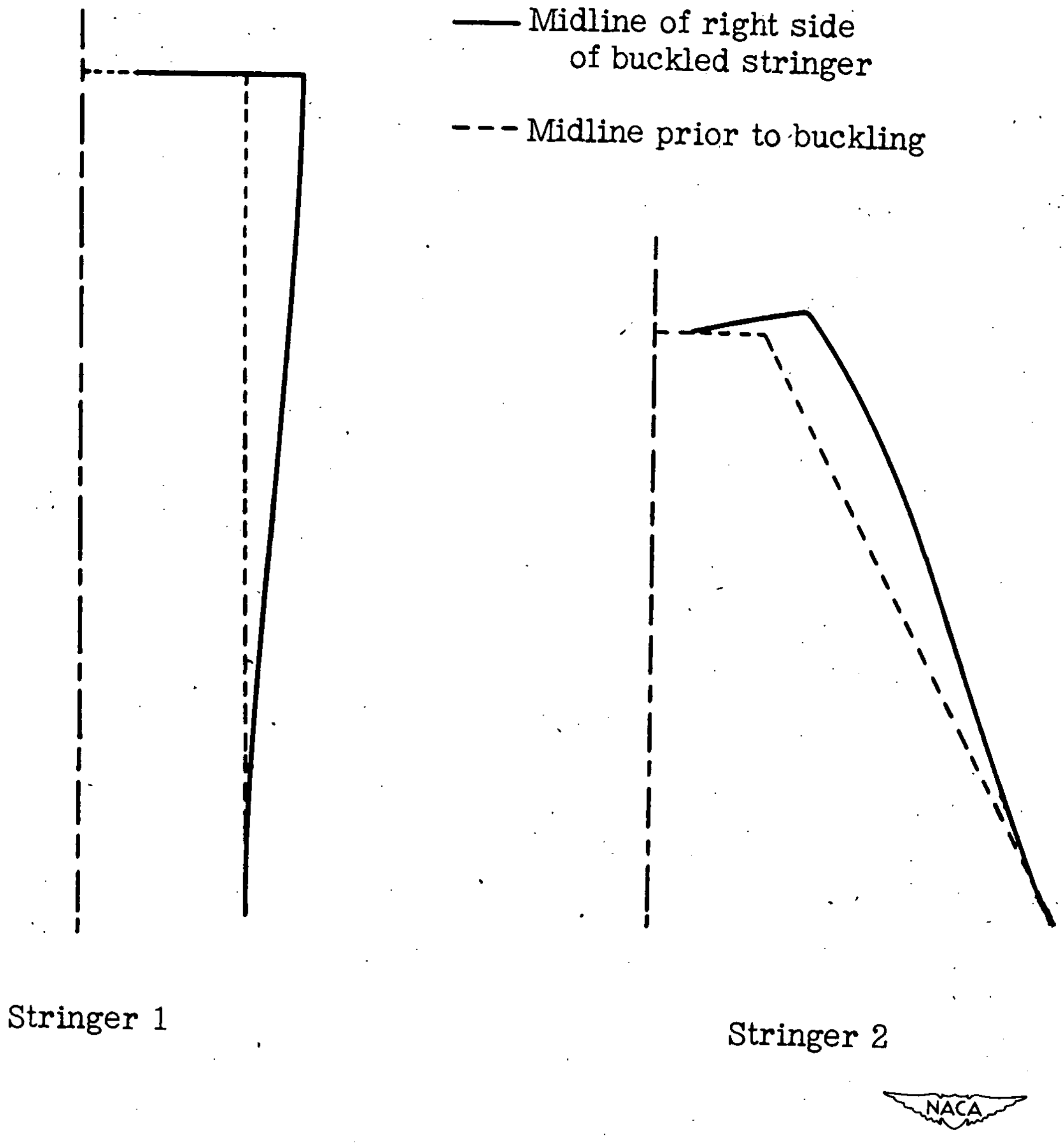

Figure 5.- Lateral deflection shapes of right sides of stringers 1 and 2 (two-parameter strain-energy method; side walls clamped at root).

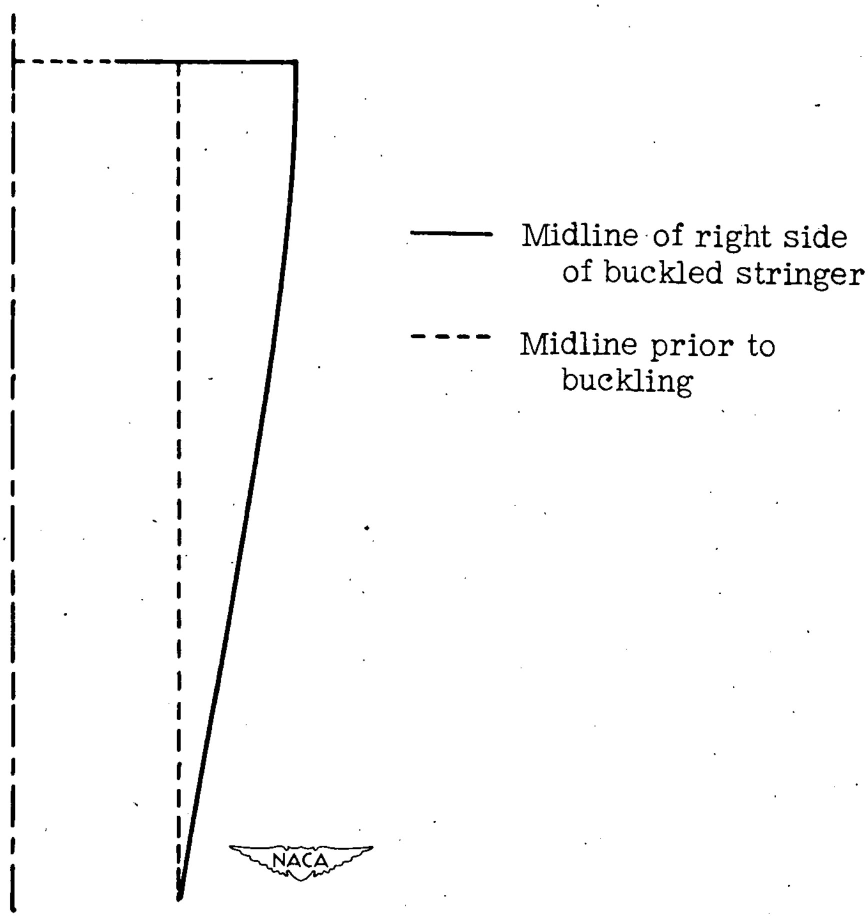

Figure 6.- Deflection shape of right side of stringer 1 (five-parameter strain-energy method; side wall hinged at root).